Spectrochimica Acta Part A: Molecular and Biomolecular Spectroscopy 124 (2014) 404–415

Contents lists available at ScienceDirect

Spectrochimica Acta Part A: Molecular and Biomolecular Spectroscopy

journal homepage: www.elsevier.com/locate/saa

Spectral, electrochemical, thermal, DNA binding ability, antioxidant and antibacterial studies of novel Ru(III) Schiff base complexes

Ayman A. Abdel Aziz [a,b,*], Hemmat A. Elbadawy [a,c]

[a] Department of Chemistry, Faculty of Science, University of Tabuk, Tabuk 71421, Saudi Arabia
[b] Department of Chemistry, Faculty of Science, Ain Shams University, Cairo 11566, Egypt
[c] Department of Chemistry, Faculty of Science, Alexandria University, Alexandria 21641, Egypt

HIGHLIGHTS

- Novel Ru(III)-NOON Schiff bases complexes.
- Spectral, electrochemical and thermogravimetric studies.
- Binding ability of Ru(III) complexes with calf thymus DNA.
- Antioxidant activity of the novel complexes.
- Antibacterial screening.

GRAPHICAL ABSTRACT

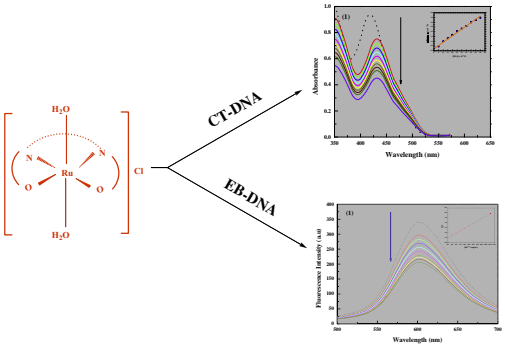

ARTICLE INFO

Article history:
Received 13 October 2013
Received in revised form 21 December 2013
Accepted 8 January 2014
Available online 22 January 2014

Keywords:
Ru(III) complexes
Characterization
Cyclic voltammetry
CT-DNA binding
Antioxidant activity
Antibacterial activity

ABSTRACT

Four new air stable low spin Ru(III) complexes of the type $[Ru(L^{1-4})(H_2O)_2]Cl$ have been synthesized, where L = dianion of the tetradentate Schiff base ligands namely N,N′bis(salicylaldehyde)4,5-dimethy-l,2-phenylendiammine (L^1H_2), N,N′bis(salicylaldehyde)4,5-dichloro 1,2-phenylendiammine (L^2H_2), N,N′bis(o-vanillin)4,5-dimethy-1,2-phenylendiammine (L^3H_2) and N,N′bis(o-vanillin)4,5-dichloro-1,2-phenylendiammine (L^4H_2). The complexes have been fully characterized by elemental analysis, infrared spectroscopy, electronic spectroscopy, magnetic susceptibility and electron spin resonance spectroscopy. Elemental analyses and spectroscopic data have been showed that, the stoichiometries of complexes were 1:1 with an octahedral geometry for all the complexes. Thermal analysis measurements indicated that the complexes have good thermal stability. The redox behavior of the complexes has been investigated by the cyclic voltammetric technique. The interaction of these complexes with calf thymus DNA (CT-DNA) was explored by different techniques which revealed that the complexes could bind to CT-DNA through an intercalative mode. Furthermore, the antioxidant activity of the Ru(III) complexes against superoxide and hydroxyl radicals was evaluated by using spectrophotometer methods *in vitro*. The experiments on antioxidant activity show that the complexes were found to possess potent antioxidant activity. Additionally, as a potential application the antibacterial activity of the complexes was assessed by testing their effect on the growth of various strains of bacteria.

Introduction

Interactions between small molecules and DNA rank among the primary action mechanism of anticancer activity and designing of molecules that bind and cleave DNA have attracted extensive

* Corresponding author at: University of Tabuk, Tabuk 71421, Saudi Arabia. Tel.: +966 0595216274.
E-mail addresses: aabdelaziz@ut.edu.sa, aymanaziz31@gmail.com (A.A. Abdel Aziz).

1386-1425/$ - see front matter © 2014 Elsevier B.V. All rights reserved.
http://dx.doi.org/10.1016/j.saa.2014.01.050

attention [1–4]. Additionally, it has been demonstrated that free radicals can damage proteins, lipids, and DNA of bio-tissues, leading to increased rates of cancer [5]. Fortunately, antioxidants can prevent this damage, due to their free radical scavenging activity [6]. Hence, it was very important to develop compounds with both strong antioxidant and DNA-binding properties for effective cancer therapy. Transition metal complexes of Schiff bases have been widely exploited to develop synthetic binding and cleavage agents for DNA [7–9].

Ruthenium's properties are well suited towards pharmacological oxidation states (II–IV) under physiologically relevant conditions [10]. Also, the energy barrier for interconversion between these oxidation states is relatively low, allowing for ready oxidation state changes when inside the cell [11]. Furthermore, ruthenium tends to form octahedral complexes, which gives the chemist two more ligands to exploit compared with platinum(II) complexes, which adopt a square planar geometry and can also form strong chemical bonds with a range of different elements of varying chemical 'hardness' and electronegativities, meaning that ruthenium can bind to a range of biomolecules, not just DNA [12].

Ru(II) and Ru(III) complexes are presently an object of great attention in the field of medicinal chemistry, as antitumor agents with selective antimetastatic properties and low systemic toxicity. Ruthenium compounds appear to penetrate reasonably well the tumor cells and bind effectively to DNA [13,14].

The well-developed synthetic chemistry of ruthenium, particularly with imine ligands provides for many approaches to innovative new metallopharmaceuticals [15]. Advantages of utilizing ruthenium imine complexes in drug development include; (i) reliable preparations of stable complexes with predictable structures, (ii) the ability to tune ligand affinities, electron transfer, substitution rates, and reduction potentials, and (iii) an increasing knowledge of the biological effects of ruthenium complexes.

However little work was focused on binding ability and antioxidant activity of ruthenium(III) Schiff bases complexes and as a result of the continuing quest for new complexes of ruthenium, in this work, we are reporting the synthesis, spectral and electrochemical characterization of a series of new Ru(III) complexes containing tetradentate Schiff base ligands derived from condensation reactions of 4,5-dimethyl-1,2-phenylendiammine and 4,5-dichloro-1,2-phenylendiammine with salicylaldehyde and o-vanillin. Furthermore, the interaction of calf thymus DNA (CT-DNA) with the novel Ru(III) complexes was investigated by UV–Vis. Spectrophotometry, fluorescence quenching and viscosity measurements. Furthermore, the antioxidant activity of the complexes was determined by superoxide and hydroxyl radical scavenging method *in vitro*. In addition, the antibacterial activity of the reported compounds was studied and the results were compared with standard antibiotics.

Experimental

Materials

4,5-Dimethyl-1,2-phenylendiammine, 4,5-dichloro-1,2-phenylendiammine, o-vanillin, salicylaldehyde and $RuCl_3{\cdot}3H_2O$ were supplied from Aldrich. Calf thymus DNA (CT-DNA) and ethidium bromide (EB) were purchased from Sigma Chemicals Co. All solvents used were of analytical reagent grade and used without further purification.

Instruments

Carbon, hydrogen and nitrogen were determined using Perkin Elmer 2400 CHN elemental analyzer. Ruthenium content of the complexes was estimated by using 1-nitroso-2-naphthol reagent [16] by adopting spectrophotometric extraction technique [17]. The chloride content of the complexes was determined by photometric method [18]. The FT-IR spectra of the samples in the 4000–400 cm^{-1} region were obtained in KBr discs on a Unicam-Mattson 1000 FT-IR. The molar conductivities of the complexes (1×10^{-3} M) in dimethylformamide (DMF) solution were measured at room temperature by using Jenway 4010 conductivity meter. Room temperature (298 K) magnetic susceptibilities were measured using a Sherwood Scientific balance using $Hg[Co(SCN)_4]$ as a calibrant. Diamagnetic corrections calculated from Pascal's constants [19] were used to obtain the molar paramagnetic susceptibilities. Electron spin resonance (ESR) measurements of solid state Ru(III) complexes were recorded at room temperature (298 K) and liquid nitrogen temperature (77 K) on Bruker EPR spectrometer at 9.706 GHz (X-band), the microwave power was (1.0 mW) with 4.0 G modulation amplitude, using 2,2-diphenylpyridylhydrazone (DPPH) as standard ($g = 2.0037$). Cyclic voltammetric measurements were carried out using a Princeton EG and GPARC model potentiostat using glassy carbon working electrode and all the potentials were referred to Ag/AgCl. Thermogravimetric analyses (TGA) were carried out using a Shimadzu DT-50 thermal analyzer under nitrogen atmosphere with a heating rate 10 °C/min. The UV–Vis spectra were recorded on a Shimadzu UV 1800 spectrophotometer. Fluorescence spectra were recorded on a Jenway 6270 fluorimeter at room temperature.

Syntheses

Microwave assisted solvent-free synthesis of the Schiff base ligands ($L^{1-4}H_2$)

The ligands $L^{1-4}H_2$ were previously synthesized by Ref. [20]. However, microwave assisted solvent-free synthesis method is used to enhance the yield and reduce the time. 0.1 mol of the diamine derivative and 0.2 mol of aldehyde were mixed well in a 50 ml Pyrex beaker and the mixture was irradiated in a microwave oven for one minute. The yellow product obtained was separated, dried and recrystallized from ethanol and the purity of the ligands was checked by TLC.

Synthesis of Ru(III) complexes (1–4)

All Ru(III) complexes were synthesized according to the general procedure: a stoichiometric amount of $RuCl_3{\cdot}3H_2O$ (10 mmol) in ethanol was added to a hot ethanol solution of the desired ligand (10 mmol) and the reaction mixture was boiled under reflux with stirring for 3 h. On cooling the desired complex was obtained as powder. In some cases, complete precipitation was achieved by the addition of diethyl ether to the cold reaction mixture. The solvent was evaporated on a vacuum line. The residue was washed several times with hot petroleum ether (60–80 °C) and recrystallized from benzene/ethanol to give reddish-brown crystals. The products were finally dried *in vacuo* over P_2O_5. Synthetic route of $[Ru(L^{1-4})(H_2O)_2]Cl$ complexes (1–4) is shown in Scheme 1.

DNA-binding studies

All experimental involving CT-DNA were performed in HCl/NaCl (5:50 mM) buffer solution (pH = 7.24). *Tris*–HCl was prepared using deionized and sonicated triple distilled water and kept at 4 °C for 3 days. The absorption ratio of CT-DNA solutions A_{260}/A_{280} was 1.8:1.9, indicating that the CT-DNA was sufficiently free from protein [21]. The CT-DNA concentration was determined via absorption spectroscopy using the molar absorption coefficient of 6600 M^{-1} cm^{-1} (260 nm) [22]. Stock solutions of metal complexes were prepared by dissolving them in dimethylformamide (DMF) and suitably diluting them with the corresponding buffer to the required concentrations for all experiments. The extent of DMF

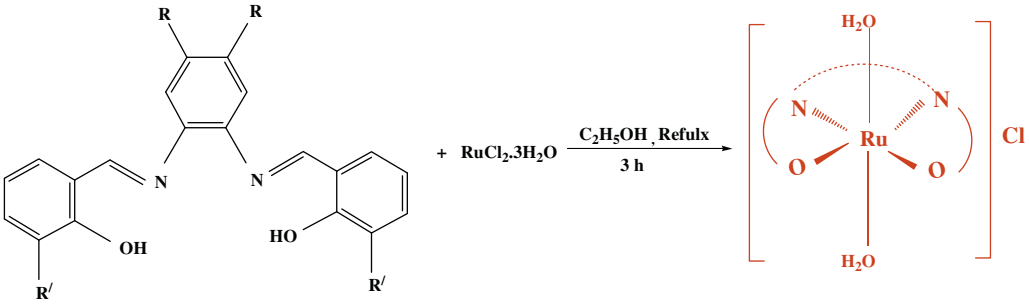

R= CH_3 and R′ = H — H_2L^1
R= Cl and R′ = H — H_2L^2
R= CH_3 and R′ = OCH_3 — H_2L^3
R= Cl and R′ = OCH_3 — H_2L^4

Scheme 1. Synthetic route of $[Ru(L^{1-4})(H_2O)_2]Cl$ complexes (1–4).

in the final concentration did not exceed 0.1% in the tested solutions. At this concentration, DMF was not found to have any effect on DNA conformation.

Electronic absorption spectroscopy

Electronic absorption titration experiments were performed with fixed Ru(III) complex concentration (10 μM), while gradually increasing the concentration of CT-DNA (5.0–50.0 μM). When measuring the absorption spectra, an equal amount of CT-DNA was added to both the complex solutions and the reference buffer solution to eliminate the absorbance of CT-DNA itself. The absorbance values were recorded after each successive addition of CT-DNA solution and equilibration for ~5 min. Each sample was measured three times and an average value was calculated. The intrinsic binding constant K_b of Ru(III) complexes with CT-DNA was determined using the following equation [22]:

$$\frac{[DNA]}{(\varepsilon_a - \varepsilon_f)} = \frac{[DNA]}{(\varepsilon_b - \varepsilon_f)} + \frac{1}{K_b(\varepsilon_b - \varepsilon_f)} \quad (1)$$

where [DNA] is the concentration of DNA in base pairs, ε_a is the extinctions coefficient observed for the for the MLCT absorption band at the given DNA concentration, ε_f is the extinction coefficient of the free complex in solution and ε_b is the extinction coefficient of the complex when fully bound to DNA. A plot of $[DNA]/[\varepsilon_a - \varepsilon_f]$ versus [DNA] gave a slope of $1/(\varepsilon_a - \varepsilon_f)$ and Y intercept equal to $(1/K_b)(\varepsilon_b - \varepsilon_f)$. The intrinsic binding constant (K_b) is given by the ratio of the slope to the intercept.

Fluorescence spectroscopy

Further support for binding of Ru(III) complexes to CT-DNA was studied through competitive emission quenching experiment. Ethidium bromide (EB) is a common fluorescent probe for DNA structure and has been employed in examinations of the mode and process of metal complexes binding to DNA [23]. EB shows weak reduced fluorescence intensity in buffer because of quenching by solvent molecules, but its fluorescence is enhanced when bound to DNA because of its intercalation into the helix and it is quenched by the addition of another molecule that displaces EB from DNA [24]. A 2.0 mL solution of 4 μM DNA and 0.32 μM EB (at saturating binding levels) was titrated by 2.5–25.0 μM the complexes and ligand. Quenching data were analyzed according to the Stern–Volmer equation which could be used to determine the fluorescent quenching mechanism:

$$I_o/I = 1 + K_q[Ru^{(III)}\ \text{complex}] \quad (2)$$

where I_o and I are the fluorescence intensities in the absence and presence of Ru(III) complex, respectively. Plots of I_o/I versus [$Ru^{(III)}$ complex] appear to be linear and K_q depends on temperature [25].

Viscosity measurements

Viscosity measurements were carried out using an Ostwald's capillary viscometer, immersed in a thermo stated water bath with the temperature setting at 25 ± 0.1 °C. CT-DNA samples with an approximate average length of 200 base pairs were prepared by sonication in order to minimize complexities arising from DNA flexibility [26]. Titrations were performed for the complexes (0.0–5.0 μM), and each compound was introduced into a DNA solution (0.30 mM) present in the viscometer. The flow times were measured with a digital stopwatch. Each sample was measured three times and an average flow time. The data were presented as $(\eta/\eta_o)^{1/3}$ versus [Ru(III) complex]/[DNA] ratio of the concentration of the compound [27], where η and η_o are the viscosity of DNA in the presence and absence of the complex respectively [28,29]. The values of η and η_o were calculated by the following equation:

$$\eta = (t - t_o)/t_o \quad (3)$$

where t is the observed flow time of DNA containing solution and, t_o is the flow time of buffer alone. Relative viscosities for DNA were calculated from the relation, η/η_o.

Antioxidant activity

Superoxide radical scavenging activity

The superoxide radicals ($O_2^{-\cdot}$) were produced by the system MET/$VitB_2$/NBT [30]. The amount of $O_2^{-\cdot}$ and suppression ratio for $O_2^{-\cdot}$ can be calculated by measuring the absorbance at 560 nm, because NBT can be reduced quantitatively to blue formazan by $O_2^{-\cdot}$. The solution of MET, $VitB_2$ and NBT were prepared with 0.067 M phosphate buffer (pH = 7.8) at the condition of avoiding light. The tested Ru(III) complexes were dissolved in DMF. The reaction mixture contained MET (0.01 mol L^{-1}), NBT (4.6×10^{-5} mol L^{-1}), $VitB_2$ (3.3×10^{-6} mol L^{-1}), phosphate buffer solution (0.067 mol L^{-1}) and a final concentration of Ru(III) complex from 0.03 to 1.5 μM. After incubating at 30 °C for 10 min and illuminating with a fluorescent lamp for 3 min, the absorbance (A_i) of the samples was measured at 560 nm. The sample without the tested compound and avoiding light was used as the control. The suppression ratio for $O_2^{-\cdot}$ was calculated from the following expression:

$$\text{Suppression ratio } (\%) = \frac{A_o - A_i}{A_o} \times 100 \quad (4)$$

where A_i, the absorbance in the presence of the ligand or its complexes; A_o, the absorbance in the absence of the ligand or its complexes.

Hydroxyl radical scavenging activity

The hydroxyl radical ($HO^{\cdot}$) in aqueous media was generated through the Fenton reaction [31]. The solution of the tested compounds was prepared with DMF. The reaction mixture contained 2.5 mL 0.15 M phosphate buffer (pH = 7.4), 0.5 mL 114 μM safranin, 1.0 mL 945 μM EDTA-Fe(II), 1 mL 3% H_2O_2 and 30 μL of the tested complex solution (the final concentration: $C_{i(i=1-9)}$ = 0.3, 0.6, 0.9, 1.2, 1.5, 3.0, 6.0, 9.0. 12.0 and 15.00 μM). The sample without the tested compound was used as the control. The reaction mixtures were incubated at 37 °C for 60 min in a water-bath. Absorbances (A_i, A_o, A_c) at 520 nm were measured. The suppression ratio for $HO^{\cdot}$ was calculated from the following expression:

$$\text{Suppression ratio } (\%) = \frac{A_i - A_o}{A_o - A_c} \times 100 \quad (5)$$

where A_i, the absorbance in the presence of the tested compound; A_o, the absorbance in the absence of the tested compound; A_c, the absorbance in the absence of the tested compound, EDTA-Fe(II) and H_2O_2. The antioxidant activity was expressed as the 50% inhibitory concentration (IC_{50}). IC_{50} values were calculated from regression lines where: *x* was the tested compound concentration in mM and y was percent inhibition of the tested compounds.

Evaluation of antibacterial activity

In vitro antibacterial activity of ligands and their Ru(III) complexes were assessed against a series of Gram positive (*Bacillus subtilis*, *Micrococcus luteus*) and Gram negative (*Pseudomonas aeruginosa, Pseudomonas mendocina*) using agar plate disc method [32,33]. Stock solution was made by dissolving compound in 10 mL of DMSO. The media was made by dissolving nutrient agar (15 g) in 1 L distilled water. The mixture was autoclaved for 15 min at 120 °C and then dispensed into sterilized petri dishes, allowed to solidify and then used for inoculation. Target microorganisms cultures were prepared separately in 15 ml of liquid nutrient agar for activation. Inoculation was done with the help of micropipette with sterilized tips, 100 μl of activated strain was placed onto the surface of agar plate, spread over the whole surface and then two wells having diameter of 10 mm were dug in media. Sterilized stock solutions were used for the application in the well of inoculated agar plates. In this well of inoculated agar plates 100 μl of solution was poured and incubated at 37 °C for 48 h. Activity was determined by measuring the diameter of zone showing complete inhibition and has been expressed in mm. All this experiments were performed in triplicate.

Results and discussion

Characterization of the complexes

The reactions of $RuCl_3{\cdot}3H_2O$ with tetradentate Schiff bases ligands ($L^{1-4}H_2$) in a 1:1 M ratio in dry ethanol afforded new hexacoordinated low spin Ru(III) Schiff base complexes. Elemental analyses and some physical properties of the reported ligands and their Ru(III) complexes are listed in Table 1. The proposed molecular formulae for all the complexes are in good agreement with the stoichiometries concluded from their analytical data. The complexes are stable in atmospheric conditions for extended periods and easily soluble in DMF and DMSO; slightly soluble in ethanol, methanol and acetone; insoluble in benzene, water and diethyl ether. The molar conductance (Λ_m) values of the complexes in DMF (1×10^{-3} M) at 25° fall in the range 99.79–107.21 Ω^{-1} cm^2 mol^{-1} (Table 1), hence all complexes are considered as 1:1 electrolytes in nature [34] and thus may be formulated as $[Ru(L^{1-4})(H_2O)_2]Cl$.

FT-IR spectra

The most important IR bands of the reported Schiff bases and their Ru(III) complexes are listed in Table 2. On the basis of the very similar spectra of the four complexes, it may be assumed that they have the similar coordination structures. The IR spectra of Schiff bases exhibited a broad band of medium intensity at 3389–3444 cm^{-1}, strong band at 1608–1617 cm^{-1}, and a medium band at 1274–1279 cm^{-1}, which were assigned to H-bonded —OH stretching ν(OH), azomethine ν(C=N) group and phenolic oxygen ν(C—O) group vibrations respectively. In comparison with the spectra of the Schiff bases, the ν(C=N) band exhibit downward shift in the range 1605–1613 cm^{-1} in the FT-IR spectra of the complexes, which is in accordance with the coordination of the azomethine function to the metal ion for all the complexes [35]. Furthermore, on complexation, the medium band corresponding to phenolic oxygen ν(C—O) is shifted to higher wave number in the range 1299–1334 cm^{-1} for all the complexes indicating that, the ligands coordinate through their deprotonated form and formation of metal–oxygen bonds. In addition, new bands were observed in the region 503–525 cm^{-1} and 455–480 cm^{-1}, which were assigned to the formation of Ru—O and Ru—N bonds respectively [36] which further supports the coordination of the azomethine nitrogen and the phenolic oxygen. Finally, the presence of coordinated water was suggested by the very broad absorption

Table 1
Yield %, molecular weight, microanalysis and conductivity data of the reported Schiff bases ligands ($L^{1-4}H_2$) and their Ru(III) complexes.

Compounds	Yield (%)	M.Wt	Color	(Calc.) found (%)					Λ_m (Ω^{-1} cm^2 mol^{-1})
				C	H	N	Cl	Ru	
L^1H_2 $C_{22}H_{20}N_2O_2$	88	344.41	Yellow	(76.72) 76.21	(5.85) 5.72	(8.13) 7.98	–	–	–
$[Ru(L^1)(H_2O)_2]Cl$ (1) $[C_{22}H_{22}N_2O_4Ru]Cl$	77	514.95	Reddish brown	(51.31) 51.22	(4.30) 4.21	(5.44) 5.39	(6.88) 6.79	(19.62) 19.59	101.45
L^2H_2 $C_{20}H_{14}N_2O_2Cl_2$	89	385.24	Yellow	(62.35) 62.19	(3.66) 3.60	(7. 27) 7.25	(18.40) 18.38	–	–
$[Ru(L^2)(H_2O)_2]Cl$ (2) $[C_{20}H_{16}N_2O_4Cl_2Ru]Cl$	73	555.78	Reddish brown	(43.22) 43.10	(2.90) 2.83	(5.09) 5.00	(19.13) 19.00	(18.18) 18.02	105.70
L^3H_2 $C_{24}H_{24}N_2O_4$	94	404.46	Orange	(71.27) 71.01	(5.98) 5.77	(6.92) 6.78	–	–	–
$[Ru(L^3)(H_2O)_2]Cl$ (3) $[C_{24}H_{26}N_2O_6Ru]Cl$	82	575.00	Reddish brown	50.13 (49.99)	4.55 (4.48)	(4.87) 4.77	(6.16) 6.00	(17.57) 17.41	107.21
L^4H_2 $C_{22}H_{18}N_2O_4Cl_2$	92	445.29	Yellow	(59.34) 59.21	(4.07) 3.82	(6.29) 6.11	(15.92) 15.75	–	–
$[Ru(L^4)(H_2O)_2]Cl$ (4) $[C_{22}H_{20}N_2O_6Cl_2Ru]Cl$	74	615.84	Reddish brown	(42.90) 42.83	(3.27) 3.13	(4.54) 4.45	(17.27) 12.057	(16.41) 16.27	99.79

Table 2
The infrared (cm^{-1}) and UV–Vis. spectral data of the reported ligands ($L^{1-4}H_2$) and their Ru(III) complexes.

Compound	ν(OH)	ν(C=N)	ν(C—O)	ν(Ru—O)	ν(Ru—N)	UV–Vis λ_{max} (nm)
L^1H_2	3428(br.)	1608(s)	1274(m)	–	–	216[a], 297[b]
$[Ru(L^1)(H_2O)_2]Cl$ (1)	3381(br.)	1605(s)	1299(m)	511(w)	455(w)	285[a], 339[b], 422[c]
L^2H_2	3444(br.)	1616(s)	1279(m)	–	–	214[a], 295[b]
$[Ru(L^2)(H_2O)_2]Cl$ (2)	3398(br.)	1609(s)	1332(m)	525(w)	480(w)	284[a], 338[b], 419[c]
L^3H_2	3389(br.)	1610(s)	1276(m)	–	–	224[a], 308[b]
$[Ru(L^3)(H_2O)_2]Cl$ (3)	3324(br.)	1607(s)	1334(m)	507(w)	474(w)	281[a], 334[b], 414[c]
L^4H_2	3394(br.)	1617(s)	1278(m)	–	–	223[a], 301[b]
$[Ru(L4)(H_2O)_2]Cl$ (4)	3373(br.)	1613(s)	1329(m)	503w)	461(w)	290[a], 343[b], 423[c]

*s, strong; m, medium; w, weak; br., broad.
[a] π–π*.
[b] n–π*.
[c] Charge transfer.

band in the region 3324–3398 cm^{-1} in the IR spectra of complexes [37]. Thus, the FT-IR spectral data provide strong evidences for the complexation of the tetradentate Schiff bases with ONNO sequence. Fig. S1 represents the FT-IR spectra of H_2L^3 ligand and its Ru(III) complex.

Electronic spectra

The electronic spectra were recorded in order to obtain information about the geometry of the complexes. The electronic spectra of the free ligands and the complexes were carried out in DMF – buffer solution. The absorption region and the assignment of the absorption bands of the ligands and complexes are listed in Table 2. The electronic spectra of all the free ligands showed two types of transitions, one appeared at the range 214–224 nm which can be assigned to π–π* transitions from the benzene ring and the double bond of the azomethine group and the second bands in the 295–308 nm region are due to n–π* transition of non-bonding electrons present on the nitrogen of the azomethine group. These peaks exhibited bathochromic shift upon complex formation, which supported the coordination of the ligands to Ru(III) ion. The ground state of Ru(III) in an octahedral environment is $^2T_{2g}$ and the first excited doublet levels in the order of increasing energy are $^2A_{2g}$ and $^2T_{1g}$, which arise from $t_{2g}^4e_g^1$ configuration [38]. Hence, two bands corresponding to $^2T_{2g} \rightarrow {}^2A_{2g}$ and $^2T_{2g} \rightarrow {}^2T_{1g}$ are possible. Besides the π–π* and n–π* transitions, the UV–Vis. spectra of the reported Ru(III) complexes show a third intense absorption band in the region 414–423 nm, which can be assigned to charge transfer (CT) transitions [39], which were absent in the spectra of the respective free ligands. In a d^5 system, especially in Ru(III) which has relatively high oxidizing properties, the charge transfer bands of the type $L_{\pi y} \rightarrow T_{2g}$ are prominent in the low energy region, which obscures the weaker bands due to d–d transitions [40]. Similar observations have been made for other Ru(III) octahedral complexes [41] and in most Ru(III) Schiff base chelates [42]. Electronic spectra of Ru(III) complexes are depicted in Fig. 1.

Magnetic moment and EPR spectra

The room temperature μ_{eff} values per ruthenium ion for the reported complexes were in 1.68–1.73 BM range (Table 3). The values obtained lie in the BM range corresponding to one unpaired electron [43], which corresponds to the +3 state of ruthenium and in consistent with non-interacting low spin t_{2g}^5 ($S = 1/2$) configuration. The EPR spectra of Ru(III) complexes provide information of importance in studying the Ru(III) ion environment. The EPR spectra of all the complexes were recorded at room temperature and liquid nitrogen temperature. The 'g' values are listed in Table 3. All Ru(III) complexes exhibited EPR spectra with $g_x = g_y \neq g_z$. The

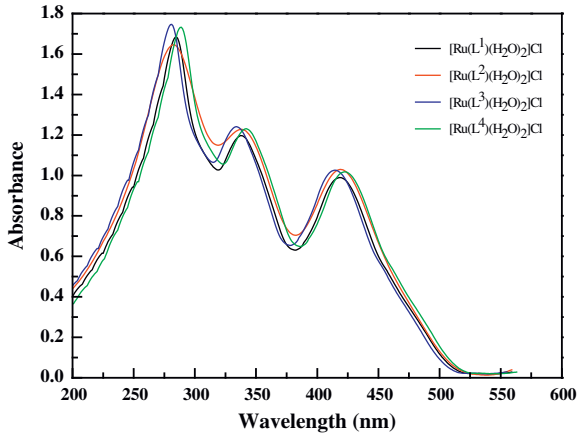

Fig. 1. UV–Vis. spectra of Ru(III) complexes.

two different 'g' values ($g_x = g_y \neq g_z$) are an indicative of a tetragonal distortion in these octahedral complexes [44]. In addition, the nature and position of the lines in the spectra of these complexes are similar to those of the other octahedral complexes [45]. The EPR spectrum of $[RuL^1(H_2O)_2]Cl$ complex at room temperature (RT) and at liquid nitrogen temperature (LNT) is depicted in Fig. 2. The spectrum of at LNT show improved resolution with the 'g' value and there is no much variation observed when compared with that observed that of RT.

Cyclic voltammetry study

The electrochemical studies of the Ru(III) complexes were carried out in acetonitrile solution, in the range +2.0 to −2.0 V using glassy carbon electrode as working electrode, Ag/AgCl as reference electrode and tetrabutyl ammonium chloride (0.1 M) as supporting electrolyte. The solution was deareated with a continuous flow of nitrogen gas for 15 min. before scanning. A respective voltammogram of the complex $[Ru(H_2O)_2(L^4)]Cl$ has been depicted in Fig. 3 and the data are given in Table 3. All the complexes are electroactive only with respect to metal center. The complexes (10^{-3} M) gave only quasi reversible cyclic voltammetric response due to Ru(III)–Ru(II) couple in the range of $E_{1/2} = -0.882$ to −0.776 V, with peak to peak separation (ΔE_p) of 0.195–0.240 V. This is attributed to slow electron transfer and adsorption of the complexes onto the electrode surface [46]. The E_{12} and ΔE_p values are in good agreement with those recently reported for other similar Ru(III) Schiff base complexes [47,48]. The E_{12} (reduction) values of the complexes containing one phenyl ring in the aldehyde part of the Schiff base ligands range from 0.52 to 0.63 V [49]. When these values are compared with that of new complexes, it has been

Table 3
EPR[a], magnetic moment and electrochemical[b] data of the reported Ru(III) complexes.

Complex	EPR parameter				μ_{eff} (BM)	$E_{pa(V)}$	$E_{pc(V)}$	ΔE_p [b] (V)	$E_{1/2}$ [c] (V)
	g_x	g_y	g_z	$(g_{av.})$[a]					
$[Ru(L^1)(H_2O)_2]Cl$ (1)	1.58	1.58	1.78	1.64	1.70	−0.785	−0.980	0.195	−0.882
$[Ru(L^3)(H_2O)_2]Cl$ (2)	1.63	1.63	1.72	1.66	1.72	−0.723	−0.963	0.240	−0.843
$[Ru(L^2)(H_2O)_2]Cl$ (3)	1.64	1.64	1.93	1.74	1.68	−0.761	−0.983	0.222	−0.872
$[Ru(L^4)(H_2O)_2]Cl$ (4)	1.61	1.62	1.81	1.68	1.73	−0.668	−0.885	0.217	−0.776

[a] $g_{av} = \left[\frac{1}{3}g_x^2 + \frac{1}{3}g_y^2 + \frac{1}{3}g_z^2\right]^{\frac{1}{2}}$.
[b] Supporting electrolyte $[NBu_4]ClO_4$ (0.1 M); scan rate, 100 mV/S; reference electrode Ag/AgCl; $\Delta E_p = E_{pa} - E_{pc}$.
[c] $E_{1/2} = 1/2\ (E_{pa} + E_{pc})$.

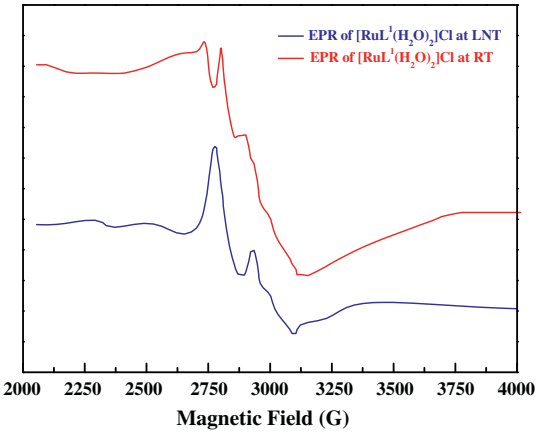

Fig. 2. EPR spectra of $[RuL^1(H_2O)_2]Cl$ complex at RT (298 K) and at LNT (77 K).

observed that the addition of one phenyl ring in the ligand causes positive shift in the E_{12} (reduction) values. This can be explained by the fact that the additional phenyl ring of electron withdrawing nature decreases the electron density around the metal center [50].

Thermogravimetric analysis

The thermal behavior of complexes under investigation was assessed using thermogravimetric analysis (TGA). The samples were analyzed in a platinum pan under N_2 and the temperature was linearly increased with a heating rate 10 °C/min over a temperature range 20–800 °C. The reported Ru(III) complexes were found to be air stable and have higher thermal stability. The TG data for the synthesized complexes are summarized in Table 4. The TG plot of the four Ru(III) complexes showed similar patterns with three resolved and well-defined decomposition steps. As an example the TG plot of $[Ru(L^2)(H_2O)_2]Cl$ exhibited a first decomposition step in the temperature range 149–256 °C with a net weight loss of 6.27% (calc. 6.48%) which has been consistent with the elimination of two H_2O molecule. The second decomposition step occurred in the temperature range 308–336 °C with a net weight loss of 32.37.00% (calc. 32.46%). This decomposition step has been assigned to the elimination of 1/2 Cl_2 and $C_6H_2Cl_2$ organic moiety. Finally the third step occurs at the temperature range 426–488 °C with a net weight loss 36.98% (calc. 37.10%) which was consistent with the loss of two (C_7H_5N) moieties to give finally RuO_2 residue with a net weight of 26.03% (calc. 25.84%). TG plot of $[RuL^2(H_2O)_2]Cl$. complexes is depicted in Fig. 4 and its thermal decomposition steps of is shown in Scheme 2.

Kinetic studies

The kinetic parameters such as activation energy (ΔE^*), enthalpy of activation (ΔH^*), entropy of activation (ΔS^*) and free energy

Table 4
Thermogravimetric characteristics of Ru(III) complexes.

Complex	Temp. range (°C)	Mass loss (%) (Calc.) found	Assignment	Residue
$[Ru(L^1)(H_2O)_2]Cl$ (1)	136–245	(6.99) 6.97	2 H_2O	RuO_2
	296–336	(27.11) 27.00	1/2 Cl_2 + C_8H_8	
	420–499	(40.05) 40.00	2 C_7H_5N	
$[Ru(L^2)(H_2O)_2]Cl$ (2)	149–256	(6.48) 6.27	2 H_2O	RuO_2
	308–336	(32.46) 32.37	1/2 Cl_2 + $C_6H_2Cl_2$	
	426–488	(37.10) 36.98	2 C_7H_5N	
$[Ru(L^3)(H_2O)_2]Cl$ (3)	182–261	(6.26) 6.19	2 H_2O	RuO_2
	324–401	(24.28) 24.14	1/2 Cl_2 + C_8H_8	
	435–506	(46.31) 45.99	2 C_8H_7NO	
$[Ru(L^4)(H_2O)_2]Cl$ (4)	187–276	(5.85) 5.72	2 H_2O	RuO_2
	333–475	(29.29) 29.11	1/2 Cl_2 + $C_6H_2Cl_2$	
	520–598	(43.24) 43.10	2 C_8H_7NO	

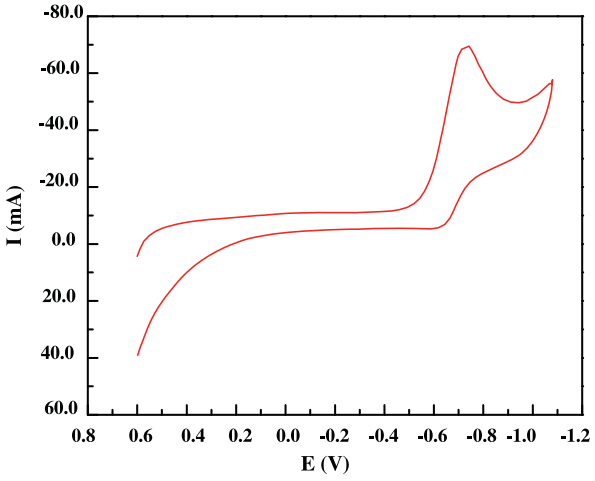

Fig. 3. Cyclic voltammogram of complex [Ru $(L^4)(H_2O)_2]Cl$.

change of the decomposition (ΔG^*) were evaluated graphically by employing the Coats–Redfern equation [51]. It is obvious from the data listed in Table 5 that all the complexes have negative entropy values indicating that activated complexes have more ordered systems than reactants.

DNA-binding studies

Previous reports [52] have suggested that ruthenium complexes can interact with DNA through three non-covalent modes such as electrostatic binding, groove binding, or intercalation. Among these interactions, intercalative binding mode is one of the most important DNA binding modes, which firstly proposed by Lerman [53]. Intercalation usually occurs when the complexes insert their

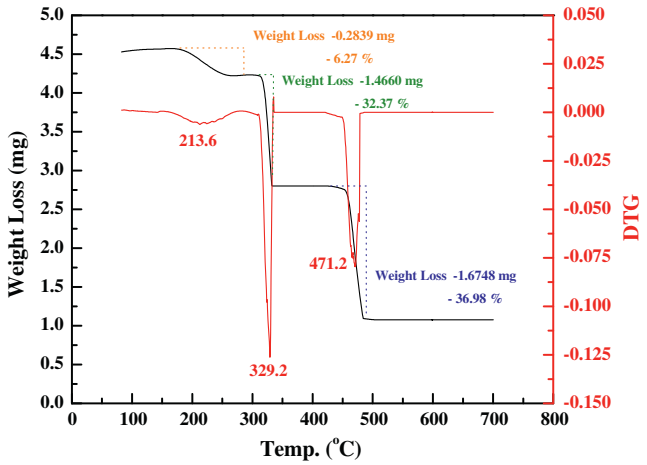

Fig. 4. TG plot of $[Ru(L^2)(H_2O)_2]Cl$ complex.

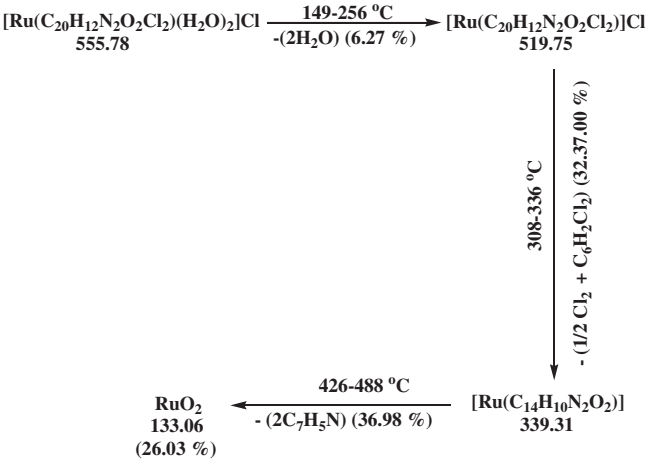

Scheme 2. Thermal decomposition steps of $[Ru(L^2)(H_2O)_2]Cl$ complex.

planar aromatic ligand between DNA base pairs. Changes in the structure of intercalative ligand could be used to attain diverse DNA binding mode of ruthenium complexes, which would result in the changes in the DNA-binding behavior, photophysical properties, excited state reactivity and biological activities of the complexes.

Electronic absorption studies

The binding modes of complexes to DNA are characterized classically through electronic absorption titrations method [54]. In the intercalative binding mode, the π^* orbital of the intercalated ligand can couple with the π orbital of the DNA base pairs, thus, decreasing the $\pi \rightarrow \pi^*$ transition energy and resulting in the bathochromism. On the other hand, the coupling π orbital is partially filled by electrons, thus, decreasing the transition possibilities and concomitantly resulting in the hypochromism [55]. Generally, the hypochromism and/or significant bathochromism in the absorption spectra arise from the strong stacking interaction between the aromatic chromophore of the ligand and DNA base pairs and the extent of hypochromism and bathochromism commonly consistent with the strength of the intercalative interaction [56].

The UV–Vis titrations of Ru(III) complexes (1–4) with CT-DNA were done in DMF-Tris buffer medium in the wave length range of 200–800 nm. It was obviously that, the absorption band appeared at 414–423 nm, which was obviously charge transfer in origin showed significant hypochromism with a red shift of 13 nm, 9 nm, 6 nm and 4 nm for complexes (1–4) respectively, suggesting that the complexes used in this study showed strong binding to DNA in an intercalative mode. The electronic absorption spectra of all the complexes in the absence and presence of CT-DNA, using a constant concentration of the complex (10 μM) are shown in Fig. 5. The extent of hypochromism was 49.10% for complex 1, 42.10% for complex 2, 37.35% for complex 3, 31.6% for complex 4.

In order to compare quantitatively the binding strength of the complexes was calculated using Eq. (1). The K_b values were $8.723 \times 10^4\ M^{-1}$ for complex 1, $6.354 \times 10^4\ M^{-1}$ for complex 2, 4.567×10^4, for complex 3, and $4.421 \times 10^4\ M^{-1}$ for complex 4 respectively, revealing that 1 > 2 > 3 > 4 in binding to CT-DNA.

This order can be explained as follows, by the methoxy in the backbone of Schiff bases 3 and 4 severe steric constraints near the core of Ru(III) when the complex intercalates into the DNA base pairs. The methoxy groups may come into close proximity of base pairs at the intercalation sites, which prevent the complexes 3 and 4 from intercalating effectively, compared to the complexes 1 and 2.

Competitive studies with EB

Further proof for the binding of Ru(III) complexes to DNA were given by carrying out studying steady-state competitive binding experiments using complexes (1–4) as quenchers were undertaken to get further proof for the binding of the complexes to DNA. The fluorescence measurement for Ru(III) complexes showed that no

Table 5
Thermodynamic parameters for the thermal degradation of Ru(III) complexes.

Complex	T_s^*	E^* (kJ mol^{-1})	A (s^{-1})	ΔH^* (kJ mol^{-1})	ΔS^* (J mol^{-1} K^{-1})	ΔG^* (kJ mol^{-1})
$[Ru(L^1)(H_2O)_2]Cl$ (1)	201	43.65	3.07×10^9	55.15	−30.25	67.62
	302	72.07	5.44×10^{11}	76.86	−72.26	86.82
	455	156.9	7.64×10^7	121.70	−145.60	143.9
$[Ru(L^2)(H_2O)_2]Cl$ (2)	213.6	68.14	6.73×10^5	58.38	−65.16	74.47
	329.2	162.6	1.97×10^{11}	186.70	−165.90	185.70
	471.2	186.74	9.04×10^6	215.90	−205.60	225.7
$[Ru(L^3)(H_2O)_2]Cl$ (3)	212	77.62	1.89×10^7	75.56	−56.35	97.45
	315	175.00	4.63×10^{13}	173.70	−117.60	98.56
	488	222.9	5.73×10^{10}	203.60	−147.3	193.70
$[Ru(L^4)(H_2O)_2]Cl$ (4)	234	73.15	3.05×10^9	73.06	−63.98	58.59
	399	173.9	5.27×10^{13}	86.75	−132.6	101.2
	564	203.5	6.09×10^6	116.00	−193.200	162.50

* T_s: the derivative peak temperature.

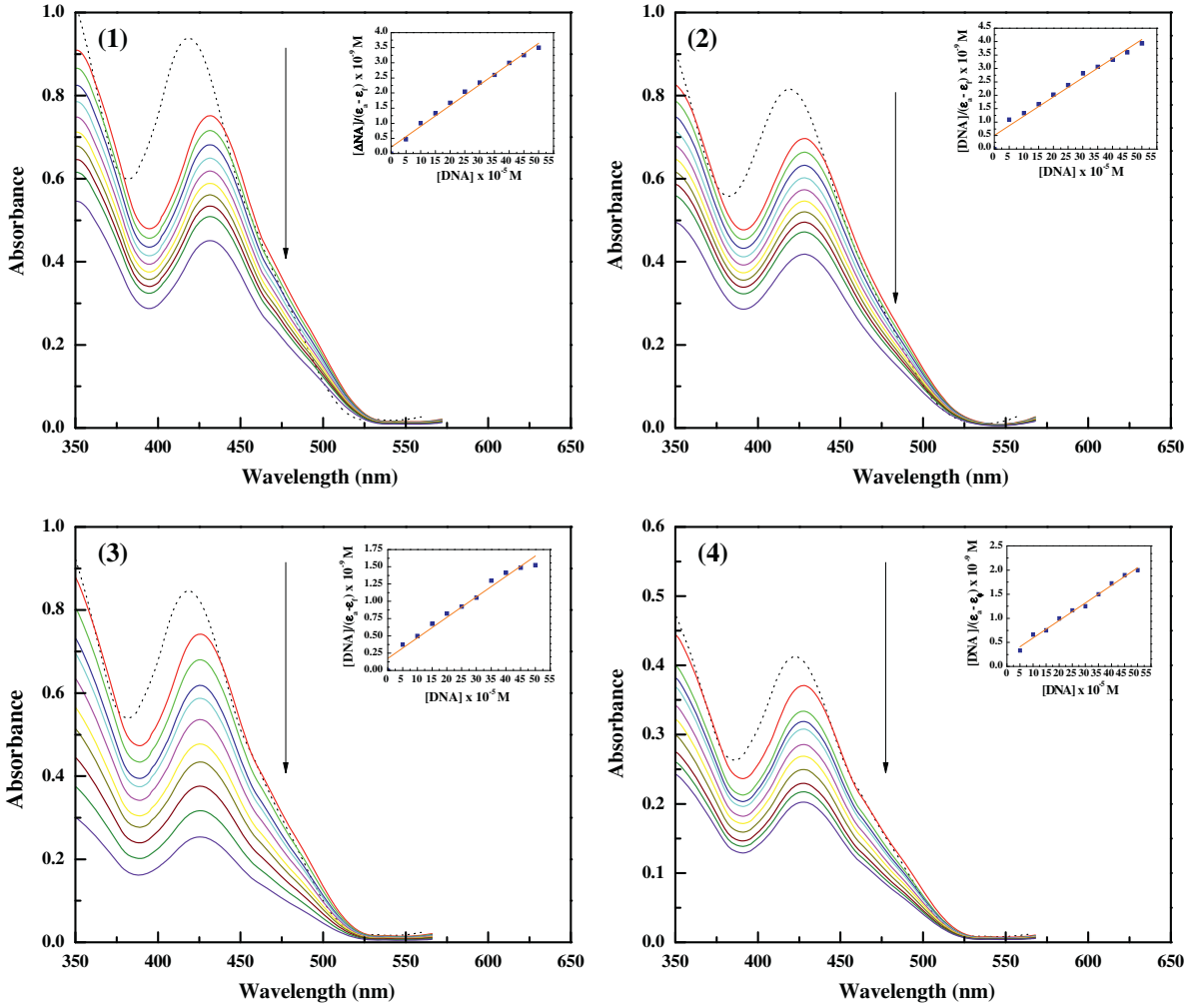

Fig. 5. Absorption spectra of Ru(III) complexes (1–4) (10 μM) in the absence and (·····) and presence (—) of CT-DNA 5,10, 15, 20, 25, 30, 35, 40, 45 and 50 μM of CT-DNA. An arrow indicates the changes in absorbance with respect to an increase of DNA concentration (inset: plot of [DNA] versus [DNA]/($\varepsilon_a - \varepsilon_f$)).

emission band either with or without CT-DNA at ambient temperature. The fluorescence quenching spectra of DNA-bound EB at 602 nm by variable complex concentrations are shown in shown in Fig. 6. Upon the addition of complexes, a significant decrease in the fluorescence intensity of the EB-DNA system occurred, which gave an indication of the binding of the Ru(III) complexes to DNA. These results indicate that Ru(III) complex could partially displace EB from the DNA-EB system, as often observed in intercalative complex-DNA modes.

The fluorescence quenching of EB bound to DNA by the complexes (1–4) is plotted against [Ru(III) complex]/[DNA] values and it was found to be in agreement with the Stern–Volmer equation (Fig. 6 insets). From the slope I_o/I versus [$Ru^{(III)}$ complex]/[DNA]-values plot using Eq. (2), The Stern–Volmer constant (K_q) was calculated. The (K_q) value give an indication about the degree of interaction the Ru(III) complexes to CT-DNA. The obtained K_q values corresponding to Ru(III) complexes (1–4) were found to be $6.583 \times 10^3\ M^{-1}$, $5.868 \times 10^3\ M^{-1}$, 4.235×10^3 and $3.174 \times 10^3\ M^{-1}$ respectively. These values indicated that, complex 1 showed highest binding ability with CT-DNA.

Viscosity studies

Optical or photophysical investigations are necessary but not sufficient to establish the mode of binding between metal complexes and DNA. Hydrodynamic measurements, i.e. viscosity and sedimentation that are sensitive to length changes are regarded as the least ambiguous and most critical tests to a binding model in solution in the absence of crystallographic structural data [57]. Viscosity measurements are proved to be least ambiguous to support a complex-DNA binding model, as these measurements are very much sensitive to length change [58]. When a small molecule intercalate between the DNA base pairs, it unwinds the DNA helix and hence increases lengthen it, resulting in significant increase in the viscosity of DNA solution. However, a partial and/or non-classical intercalation of ligand may bend (or kink) the DNA helix, resulting in the decrease of its effective length and, concomitantly its viscosity [59]. The binding of the complexes with CT-DNA was further elucidated by measuring the relative specific viscosity of DNA after the addition of varying concentration of complexes. The effect of Ru(III) complexes (1–4) on the viscosity of rod-like CT-DNA at 25 ± 0.1 °C is shown in Fig. 7. Viscosity experimental results clearly showed that the relative viscosity of CT-DNA increases steadily on addition of increasing concentration of the complexes (1–4).The increased degree of viscosity, which may depend on its affinity to DNA follows the order of 1 > 2 > 3 > 4. This observation can be explained on the fact that, classical intercalation model demands that the DNA helix must lengthen as base pairs are separated to accommodate the binding complexes, leading to the increase of DNA viscosity, as for the behaviors of the known DNA intercalators.

Antioxidant activity

As a result of the fact that, Ru(III) complexes exhibited good DNA binding affinity, it is considered worthwhile to investigate their antioxidant activity. Reactive oxygen species (ROS), such as superoxide anion ($O_2^{-\cdot}$) and hydroxyl radical ($HO^{\bullet}$), are generated by all aerobiccells during normal oxygen metabolism, and cumulative information obtained has proved that the oxidation induced by ROS is involved in the pathogenesis of various diseases through direct effects on DNA directly and by acting as antitumor promoter [60–62].

The inhibitory effects on the superoxide radical are increased for greater concentrations of Ru(III) complexes, ranging from 0.03 to 1.5 μM as shown in Fig. 8a. It is noteworthy that the scavenging effect of the four complexes is comparable at the concentration of 1.5 μM, with a measured value of approximately 90%. These results indicate that the four complexes will show almost the same activities when the concentration of complexes is as high as 1.5 μM and the differences can only be seen in low concentrations (<1.5 μM). However, in our tested concentration, activities of four complexes are also in the order of 1 > 2 > 3 > 4, with the IC_{50} value of 0.079, 0.140, 0.194 and 0.238 μM).

The scavenging abilities of the four Ru(III) complexes against hydroxyl radicals were tested as a function of concentration, ranging from 0.3 to 15 μM, shown in Fig. 8b. It can be seen that the inhibitory effects of complexes on the hydroxyl radical are related to concentration and saturate at a concentration of 9 μM. Obviously, the scavenging activities of four Ru(III) complexes follow the order of 1 (IC_{50} = 2.42) > 2 (IC_{50} = 4.28) > 3 (IC_{50} = 9.00) > 4 (IC_{50} = 42.00). The relatively small standard deviations (SD) listed in Tables 6 and 7 provide evidence of the reliability in our experimental conditions using the Fenton system to generate hydroxyl radicals.

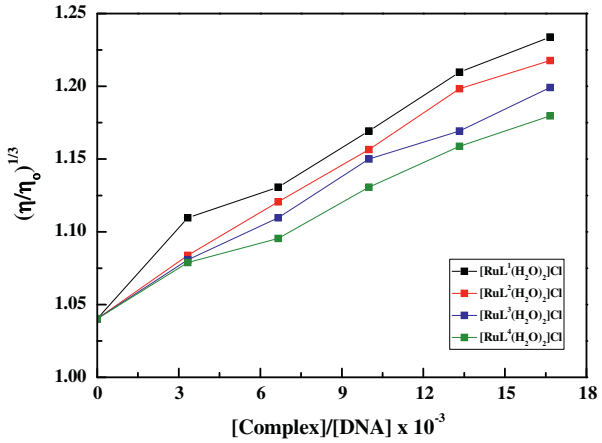

Fig. 7. Effect of increasing amounts of Ru(III) complexes on the relative viscosity at 25 (±0.1) °C of calf thymus DNA (0.30 mM).

Compared to inhibitory effects on the hydroxyl radical (Fig. 9), the four Ru(III) complexes exhibit greater activity (lower IC_{50} value) on the superoxide radical, which may be due to the higher activity of the hydroxyl radical than the superoxide radical. Considering the mononuclear structure of the four complexes, differences in the ligand structure are likely to induce variations in antioxidant activities.

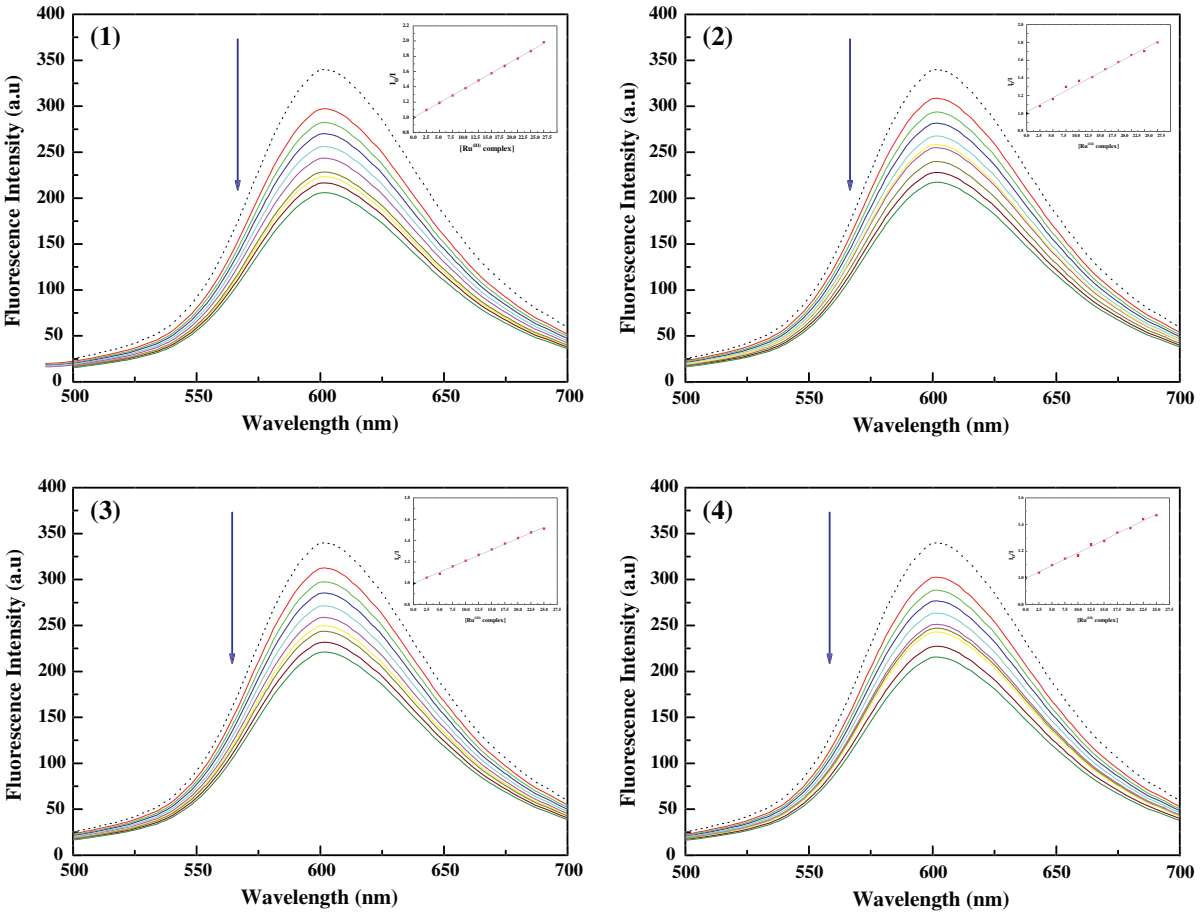

Fig. 6. Emission spectra of DNA-EB system in the absence (·····) and presence (—) of 2.5, 5.0, 7.5, 10, 12.5, 15, 17.5, 20, 22.5 and 25 μM Ru(III) complexes (1–4). An arrow indicates the changes in emission intensity upon increasing the complex concentrations. (Inset: Stern–Volmer plot of the fluorescence titration data).

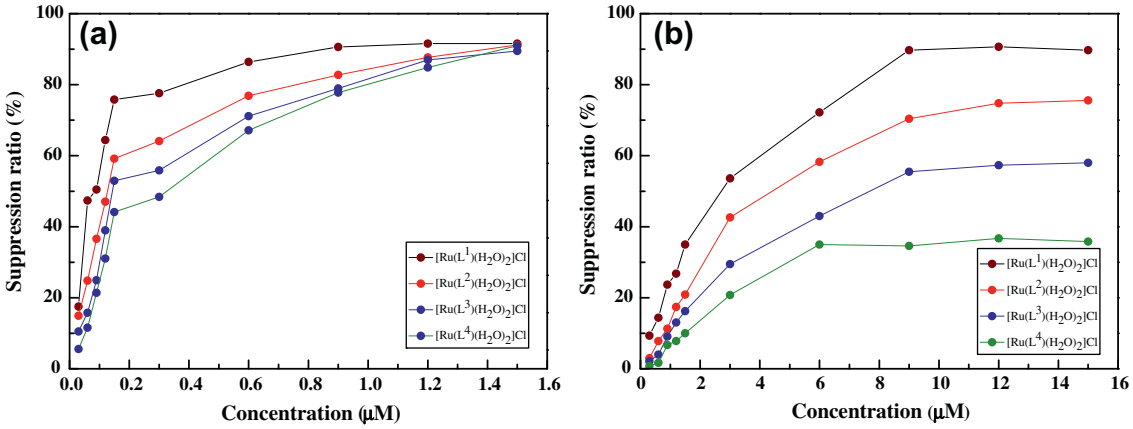

Fig. 8. The scavenging effect of Ru(III) complexes on superoxide radical (a) and hydroxyl radical (b).

Table 6
The scavenging activities of Ru(III) complexes (1–4) against superoxide radical.

Complex	Average inhibition for $O_2^{-\cdot}$ at different concentration (μM)										Equation	[a]IC_{50} (μM)	R^2
	0.03	0.06	0.09	0.12	0.15	0.3	0.6	0.9	1.2	1.5			
1	17.5	47.4	50.5	64.4	75.8	77.6	86.4	90.6	91.6	91.6	$y = 39.02x + 39.028$	0.079	0.878
2	19.2	28.6	39.8	49.7	61.2	65.9	78.0	83.6	88.3	91.6	$y = 42.895x + 86.638$	0.140	0.973
3	15.0	20.0	28.7	42.0	55.3	58.1	72.6	80.0	87.6	90.0	$y = 46.434x + 83.018$	0.194	0.972
4	10.3	16.0	25.3	34.5	46.9	51.0	68.8	78.9	85.6	91.4	$y = 49.506x + 80.901$	0.238	0.984

[a] IC_{50} values were calculated from regression lines where: x was the log of the tested complexes concentration and y was the average inhibition of the tested complexes. When the average inhibition of the tested complexes was 50%, the tested complex concentration was IC_{50}.

Table 7
The scavenging activities of Ru(III) complexes (1–4) against hydroxyl radical.

Complex	Average inhibition for $OH^{\cdot}$ at different concentration (μM)										Equation	IC_{50} (μM)	R^2
	0.3	0.6	0.9	1.2	1.5	3.0	6.0	9.0	12	15			
1	9.3	14.4	23.7	26.8	35.0	53.6	72.2	89.7	90.7	89.7	$y = 55.11x + 28.858$	2.42	0.975
2	3.0	7.8	11.3	17.4	20.9	42.6	58.3	70.4	74.8	75.6	$y = 49.39x + 18.798$	4.28	0.971
3	2.1	4.0	9.1	13.0	16.2	29.5	43.0	55.5	57.3	58.0	$y = 38.12x + 13.630$	9.00	0.968
4	0.8	1.7	6.7	7.8	10.0	20.8	35.0	34.6	36.7	35.8	$y = 25.22x + 9.0087$	42.0	0.950

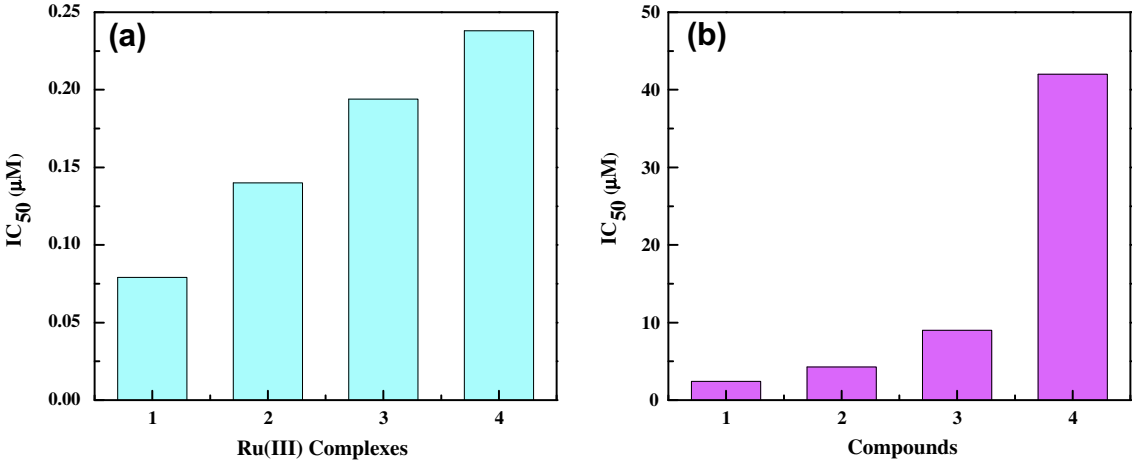

Fig. 9. Radical scavenging activity of Ru(III) complexes.

Antibacterial screening

Determination of *in vitro* antibacterial activity of the reported Schiff bases and their Ru(III) complexes are given in Table 8 and their graphical representation in Fig. 10. Antibacterial studies were done by the agar plate disc method on the following strains i.e., Gram positive *B. subtilis, M. luteus* and Gram negative *P. aeruginosa, P. mendocina* using different concentration of ligands and their complexes (50 and 100 μg/mL). Streptomycin was used as a standard drug for antibacterial activity. It may be concluded from the

Table 8
In vitro antibacterial activity of the Schiff bases ligands ($L^{1-4}H_2$) and their Ru(III) complexes.

Compound	Diameter of inhibition zone (mm)							
	(Gram +ve)				(Gram −ve)			
	R. subtilis		*M. Luteus*		*P. aeruginosa*		*P. mendocina*	
	50 (μg/mL)	100 (μg/mL)	50 (μg/mL)	100 (μg/mL)	50 (μg/mL)	100 (μg/mL)	50 (μg/mL)	100 (μg/mL)
L^1H_2	9	10	9	11	8	7	9	11
L^2H_2	5	7	6	8	5	10	5	9
L^3H_2	10	11	11	13	9	8	10	14
L^4H_2	7	9	7	10	6	11	6	10
(1)	17	18	17	20	14	17	15	18
(2)	13	15	13	17	13	15	14	16
(3)	14	20	19	22	16	19	18	21
(4)	19	17	15	19	18	16	15	18
Streptomycin	22	25	20	23	23	25	25	27

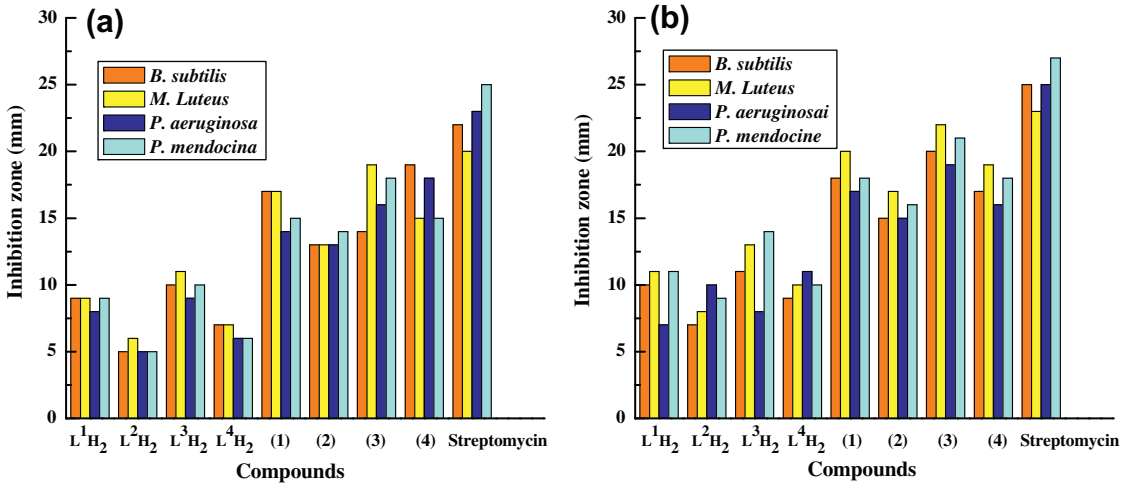

Fig. 10. Zone of inhibitions of reported compounds and antibiotic ((a) 50 μg/mL and (b) 100 μg/mL) against gram (+) and gram (−) bacteria strains.

antibacterial screening data that: (i) The antibacterial activity of ligands and their complexes was due to the presence of toxophorically important imine groups where the mode of action of these compounds may involve the formation of hydrogen bond through azomethine group with the active center of cell constituents, thereby resulting in interference with normal cell process. (ii) A marked enhancement of *in vitro* biocidal studies of the ligands was exhibited on coordination with Ru(III) ion against all microorganisms strains under tested identical experimental conditions. The increase in antibacterial activity may be explained on basis of fact that on chelation the polarity of Ru(III) ion is reduced due to overlap of ligand orbital and sharing of positive charge of ruthenium ion with donor groups. Further it increases delocalization of chelate ring and increases the lipophilicity of complexes. This increased lipophilicity enhances penetration of complexes there by disturbing the respiration process of cell and blocking the synthesis of proteins, which further restricts growth of organisms. (iii) It is evident from the data that the complexes were more toxic towards Gram (+) strains as compared to Gram (−) strains which may be attributed to the fact that the cell wall of Gram (−) strains have more antigenic properties due to the presence of an outer lipid membrane of lipopolysaccharides. (iv) Some compounds have activity close to standard drug. It was clear from the data that compounds with higher concentration were proportionately more potent as compared to same compound with higher concentration.

Conclusions

Four novel complexes of Ru(III)-tetradentate Schiff base ligands have been synthesized and structurally characterized. Based on elemental analysis, molar conductivity, UV–Vis, magnetic, EPR, FT-IR spectral data and TG analysis, mononuclear octahedral complexes of the general formula $[RuL^{1-4}(H_2O)_2]Cl$ are proposed, where L = dianion of the tetradentate Schiff base ligand. The CT-DNA binding abilities of the complexes have been studied. The results suggest that all the complexes bind to CT-DNA by an intercalative mode with different degrees. These studies form an important rationale for drug design and warrant further *in vivo* experiments and pharmacological assays. Additionally, Ru(III) complexes also exhibited excellent antioxidant ($O_2^{-\cdot}$ and $HO^{\bullet}$ radical scavengers) and antibacterial activities. Therefore, the information obtained from the present work would help in developing new potent antioxidants and therapeutic drugs to cure certain valuable diseases.

Acknowledgement

The authors would like to acknowledge financial support for this work, from the Deanship of Scientific Research (DSR), University of Tabuk, Tabuk, Saudi Arabia, under Grant No. (S141/1434).

Appendix A. Supplementary material

Supplementary data associated with this article can be found, in the online version, at http://dx.doi.org/10.1016/j.saa.2014.01.050.

References

[1] C. Metcalfe, J.A. Thomas, Chem. Soc. Rev. 32 (2003) 215–224.
[2] H.T. Chifotides, K.R. Dunbar, Chem. Res. 38 (2005) 146–156.
[3] S.S. Bhat, A.A. Kumbhar, H. Heptullah, A.A. Khan, V. Gobre, S.P. Gejji, V.G. Puranik, Inorg. Chem. 50 (2011) 545–558.
[4] O. Dömötör, C.G. Hartinger, A.K. Bytzek, T. Kiss, B.K. Keppler, E.A. Enyedy, J. Biol. Inorg. Chem. 40 (2011) 1024–1027.
[5] D. Dreher, A.F. Junod, Eur. J. Cancer 32 (1996) 30–38.
[6] W.J. Chen, P. Guo, J. Song, W. Cao, J. Bian, Bioorg. Med. Chem. Lett. 16 (2006) 3582–3585.
[7] (a) R. Vijayalakshmi, N. Kanthimathi, V. Subramanian, B.U. Nair, Biochem. Bioph. Res. Co. 271 (2000) 731–734;
(b) V.G. Vaidyanathan, T. Weyhermuller, B.U. Nair, J. Subramanian, J. Inorg. Biochem. 99 (2005) 2248–2255;
(c) B. Wang, Z. Yang, Q. Wang, T. Cai, P. Crewdson, Bioorgan. Med. Chem. 14 (2006) 1880–1888;
(d) G. Garcia-Friaza, A. Fernandez-Botello, J.M. Perez, M.J. Prieto, V. Moreno, J. Inorg. Biochem. 100 (2006) 1368–1377;
(e) Y. Li, B. Wang, Z.Yang, Spectrochim. Acta A 67 (2007) 395–401.
[8] (a) M.A. Neelakantana, F. Rusalraj, J. Dharmaraja, S. Johnsonraja, T. Jeyakumar, M.S. Pillai, Spectrochim. Acta A 71 (2008) 1599–1609;
(b) P.K. Sasmal, A.K. Patra, A.R. Chakravarty, J. Inorg. Biochem. 102 (2008) 1463–1472;
(c) X. Ma, D. Li, J. Tian, Y. Kou, S. Yan, Trans. Met. Chem. 34 (2009) 475–481;
(d) D. Qin, Z. Yang, F. Zhang, B. Du, P. Wang, T. Li, Inorg. Chem. Commun. 13 (2010) 727–729;
(e) M.S.A. Begum, S. Saha, M. Nethaji, A.R. Chakravarty, J. Inorg. Biochem. 104 (2010) 477–484.
[9] (a) N. Raman, A. Selvan, S. Sudharsan, Spectrochim. Acta A 79 (2011) 873–883;
(b) Y. Zhang, X. Wang, L. Ding, Nucleosides Nucleotides 30 (2011) 49–62;
(c) F. Arjmand, A. Jamsheera, J. Organomet. Chem. 696 (2011) 3572–3579;
(d) R.N. Patel, S.P. Rawat, M. Choudhary, V.P. Sondhiya, D.K. Patel, K.K. Shukla, D.K. Patel, Y. Singh, R. Pandey, Inorg. Chim. Acta 392 (2012) 283–291;
(e) K.R.S. Gowda, H.S.B. Naik, B.V. Kumar, C.N. Sudhamani, H.V. Sudeep, T.R.R. Naik, G. Krishnamurthy, Spectrochim. Acta A 105 (2013) 229–237;
(f) S.O. Bahaffi, A.A. Abdel Aziz, M.M. El-Naggar, J. Mol. Strut. 1020 (2012) 188–196;
(g) S.M. Pradeepa, H.S. Bhojya Naik, B. Vinay Kumar, K.I. Priyadarsini, A. Barik, T.R. Ravikumar Naik, Spectrochim. Acta A 101 (2013) 132–139;
(h) S. Tabassum, S. Amir, F. Arjmand, C. Pettinari, F. Marchetti, N. Masciocchi, G. Lupidi, R. Pettinari, Eur. J. Med. Chem. 60 (2013) 216–232.
[10] P. Schluga, C.G. Hartinger, A. Egger, E. Reisner, M. Galanski, M.A. Jakupec, B.K. Keppler, Dalton Trans. 2006 (2006) 1796–1802.
[11] I. Bratsosa, S. Jednera, T. Gianferrarab, E. Alessio, Chimia 61 (2007) 692–697.
[12] V. Brabec, Prog. Nucleic Acid Res. Mol. Biol. 71 (2002) 1–68.
[13] (a) B. Sun, J. Guan, L. Xu, B. Yu, L. Jiang, J. Kou, L. Wang, X. Ding, H. Chao, L. Ji, Inorg. Chem. 48 (2009) 4637–4639;
(b) S.S. Bhat, A.S. Kumbhar, P. Lönnecke, E. Hey-Hawkins, Inorg. Chem. 49 (2010) 4843–4853;
(c) J.F. Kou, C. Qian, J.Q. Wang, X. Chen, L.L. Wang, H. Chao, L.N. Ji, J. Biol. Inorg. Chem. 17 (2012) 81–96;
(d) M.R. Gill, J.A. Thomas, Chem. Soc. Rev. 41 (2012) 3179–3192;
(e) X.W. Liu, Z.G. Chen, L. Li, Y.D. Chen, J.L. Lu, D.S. Zhang, Spectrochim. Acta A 102 (2013) 142–149;
(f) L. Xu, N.J. Zhong, H.L. Huang, Z.H. Liang, Z.Z. Li, Y.J. Liu, Nucleosides Nucleotides 31 (2012) 575–591;
(g) S. Jing, W. Shuo, H. Yan, L. Jie, J. Liang-Nian, M. Zong-Wan, Inorg. Chem. Commun. 11 (2008) 1382–1384;
(h) S. Jing, A. Yan, Z. Li, C. Huo-Yan, H. Yan, W. Yu-Jia, M. Zong-Wan, J. Liang-Nian, J. Inorg. Biochem. 105 (2011) 149–154.
[14] (a) C.P. Tan, J. Liu, L.M. Chen, S. Shi, L.N. Ji, J. Inorg. Biochem. 102 (2008) 1644–1653;
(b) I. Ali, K. Saleem, D. Wesselinova, A. Haque, Synth. Med. Chem. Res. 22 (2013) 1386–1398;
c) G. Raja, R.J. Butcher, C. Jayabalakrishnan, Trans. Met . Chem. 37 (2012) 169–174;
(d) D. Chatterjee, H.C. Bajaj, A. Das, J. Chem. Soc., Dalton Trans. 1995 (1995) 2497–2501;
(e) O. Dömötör, C.G. Hartinger, A.K. Bytzek, T. Kiss, B.K. Keppler, E.A. Enyedy, J. Bio. Inorg. Chem. 18 (2013) 9–17;
(f) T.S. Kamatchi, N. Chitrapriya, H. Lee, C.F. Fronczek, F.R. Fronczek, K. Natarajan, Dalton Trans. 41 (2012) 2066–2077.
[15] M.J. Clarke, Coordin. Chem. Rev. 232 (2002) 69–93.
[16] A.V.S.S. Prasad, C.S.P. Sastry, J. Ind. Chem. Soc. 79 (2002) 452–454.
[17] G. Kesser, R.J. Meyer, R.P. Larsen, Anal. Chem. 38 (1966) 221–224.
[18] M. Zall, D. Fisher, Q. Gamer, Anal. Chem. 28 (1956) 1665–1668.
[19] A. Earnshaw, Introduction to Magnetochemistry, Academic Press, London, 1968.
[20] A.A. Abdel Aziz, Synth. React. Inorg. Met. Org. Chem. 41 (2011) 384–393.
[21] C.V. Kumar, E.H. Asuncion, J. Am. Chem. Soc. 115 (1993) 8547–8553.
[22] J. Marmur, J. Mol. Biol. 3 (1961) 208–218.
[23] Y.B. Zeng, N. Yang, W.S. Liu, N. Tang, J. Inorg. Biochem. 97 (2003) 258–264.
[24] R. Indumathy, S. Radhika, M. Kanthimathi, T. Weyhermuller, B.U. Nair, J. Inorg. Biochem. 101 (2007) 434–443.
[25] M.R. Efink, C.A. Ghiron, Anal. Biochem. 114 (1981) 199–227.
[26] J.B. Chaires, N. Dattagupta, D.M. Crothers, Biochemistry 21 (1982) 3933–3940.
[27] S. Satyanaryana, J.C. Dabrowial, J.B. Chaires, Biochemistry 32 (1993) 2573–2584.
[28] M. Eriksson, M. Leijon, C. Hiort, B. Norden, A. Gradsland, Biochemistry 33 (1994) 5031–5040.
[29] Y. Xiong, X.F. He, X.H. Zou, J.Z. Wu, X.M. Chen, L.N. Ji, R.H. Li, Y.J. Zhou, R.B. Yu, J. Chem. Soc., Dalton Trans. 1 (1999) 19–24.
[30] C.C. Winterbourn, Biochem. J. 18 (1979) 625–628.
[31] C.C. Winterbourn, Biochem. J. 198 (1981) 125–131.
[32] Z.H. Chohan, Chem. Pharm. Bull. 39 (1991) 1578–1580.
[33] A.U. Rahman, M.I. Choudhary, W.J. Thomsen, Bioassay Techniques for Drug Development, Harwood Academic, Amsterdam, 2001.
[34] J.A. Dean, Lange's Hand Book of Chemistry, fourth ed., McGraw-Hill, New York, 1992.
[35] (a) S. Pal, S. Pal, J. Chem. Soc., Dalton Trans. 2002 (2002) 2102–2108;
(b) M. Amirnasr, A.H. Mahmoudkhani, A. Gorji, S. Dehghanpour, H.R. Bijanzadeh, Polyhedron 21 (2002) 2733–2742.
[36] K. Nakamato, Infrared and Raman Spectra of Inorganic and Coordination Compounds, Wiley-Interscience, New York, 1971.
[37] A.A. El-Bindary, Trans. Met. Chem. 22 (1997) 381–384.
[38] C.J. Balhausen, Ligand Field Theory, McGraw-Hill, New York, 1962.
[39] (a) K. Chichak, U. Jacquemard, N.R. Branda, Coordination. Eur. J. Inorg. Chem. 2002 (2002) 357–368;
(b) R. Samanta, B. Mondal, P. Munshi, G.K. Lahiri, J. Chem. Soc., Dalton Trans. 2001 (2001) 1827–1833.
[40] G. Venkatachalam, N. Raja, D. Pandiarajan, R. Ramesh, Spectrochim. Acta A 71 (2008) 884–891.
[41] (a) S. Patra, B. Sarkar, S. Ghumaan, J. Fiedler, S. Zalis, W. Kaim, G.K. Lahiri, Inorg. Chem. 43 (2004) 6108–6113;
(b) N. Padma Priya, S. Arunachalam, A. Manimaran, D. Muthupriya, C. Jayabalakrishnan, Spectrochim. Acta A 72 (2009) 670–676;
(c) M. Muthukumar, P. Viswanathamurthi, R. Prabhakaran, K. Natarajan, J. Coord. Chem. 63 (2010) 3833–3848.
[42] R. Ramesh, S. Maheswaran, J. Inorg. Biochem. 96 (2003) 457–462.
[43] F.A. Cotton, C.W. Wilkinson, Advanced Inorganic Chemistry, third ed., Interscience Publisher, New York, 1972.
[44] S. Arunachalam, N. Padma Priya, C. Jayabalakrishnan, V. Chinnusamy, Spectrochim. Acta A 74 (2009) 591–596.
[45] R. Prabhakaran, V. Krishnan, K. Pasumpon, D. Sukanya, E. Wendel, C. Jayabalakrishnan, H. Bertagnolli, K. Natarajan, Appl. Organomet. Chem. 20 (2006) 203–213.
[46] A.W. Wallace, W.R. Murphy Jr., J.D. Peterson, Inorg. Chim. Acta 166 (1989) 47–54.
[47] R. Prabhakaran, A. Geetha, M. Thilagavathi, R. Karvembu, V. Krishnan, H. Bertagnolli, K. Natarajan, J. Inorg. Biochem. 98 (2004) 2131–2140.
[48] R. Karvembu, C. Jayabalakrishnan, N. Dharmaraj, S.V. Renukadevi, K. Natarajan, Trans. Met. Chem. 27 (2002) 631–638.
[49] S. Priyarega, M.M. Tamizh, R. Karvembu, R. Prabhakaran, K. Natarajan, J. Chem. Sci. 123 (2011) 1319–1325.
[50] T. Hashimoto, S. Hara, Y. Shiraishi, K. Natarajan, K. Shimizu, Chem. Lett. 32 (2003) 874–875.
[51] A.W. Coats, J.P. Redfern, Nature 20 (1964) 68–69.
[52] (a) E. Corral, A.C.G. Hotze, D.M. Tooke, A.L. Spek, J. Reedijk, Inorg. Chim. Acta 359 (2006) 830–838;;
(b) A.C.G. Hotze, J.A. Faiz, N. Mourtzis, G.I. Pascu, P.R.A. Webber, G.J. Clarkson, K. Yannakopoulou, Z. Pikramenou, M.J. Hannon, Dalton Trans. 24 (2006) 3025–3034;
(c) V. Brabec, O. Nováková, Drug Resist. Update 9 (2006) 111–122;
(d) N. Ljubijankić, A. Zahirović, E. Turkušić, E. Kahrović, Croat. Chem. Acta 86 (2013) 215–222.
[53] L.S. Lerman, J. Mol. Biol. 3 (1961) 18–30.
[54] J.M. Kelly, A.B. Tossi, D.J. McConnell, C.O. Uigin, Nucleic Acids Res. 13 (1985) 6017–6034.
[55] A.M. Pyle, J.P. Rehmann, R. Meshoyrer, C.V. Kumar, N.J. Turro, K.K. Barton, J. Am. Soc. Chem. 111 (1989) 3051–3058.
[56] H. Chao, W.J. Mei, Q.W. Huang, L.N. Ji, J. Inorg. Biochem. 25 (2002) 165–170.
[57] T. Biver, F. Secco, M.R. Tinè, M. Venturini, J. Inorg. Biochem. 98 (2004) 33–40.
[58] V.G. Vaidyanathan, B.U. Nair, J. Inorg. Biochem. 93 (2003) 271–276.
[59] S. Satyanarayana, J.C. Dabrowiak, J.B. Chaires, Biochemistry 32 (1993) 2573–2584.
[60] S. Satyanarayana, J.C. Dabrowiak, J.B. Chaires, Biochemistry 31 (1992) 9319–9324.
[61] R.M. Towyz, Hypertension 44 (2004) 248–252.
[62] S.S. Leonard, D. Keil, T. Mehlman, S. Proper, X. Shi, G.K. Harris, J. Ethnopharmacol. 103 (2006) 288–296.